Optical Engineering

SPIEDigitalLibrary.org/oe

Compact camera for three-dimensional profilometry incorporating a single MEMS mirror

Toshitaka Wakayama
Toru Yoshizawa

Compact camera for three-dimensional profilometry incorporating a single MEMS mirror

Toshitaka Wakayama
Toru Yoshizawa
Saitama Medical University
Department of Biomedical Engineering
Yamane, Hidaka, Saitama, Japan
E-mail: wakayama@saitama-med.ac.jp

Abstract. To overcome inherent problems with conventional three-dimensional profiling systems based on pattern-projection method, we propose incorporating a digital device, such as a single MEMS mirror in the projection optics. In this system, a projector is controlled to generate a projection pattern with an appropriate periodic structure and sinusoidal intensity distribution. The key aspect to this projection method is that sinusoidal signals are generated by a function generator; that is, the temporal sinusoidal intensity distribution is transformed from the time domain to the spatial domain. This flexible pattern-projection method permits phase-shifting techniques to be applied to industrial measurement and inspection. This apparatus is so compact as to have a dimensional size similar to a conventional digital camera [53 mm(H) × 130 mm(W) × 38 mm(D)]. Furthermore, it is lightweight (320 g) without a battery or circuit boards. Such a compact system can be used as a palm-top camera and potentially may be used in low cost measurement systems for three-dimensional profilometry. [DOI: 10.1117/1.OE.51.1.013601]

Subject terms: compact camera; three-dimensional profilometry; fringe projection method; single MEMS mirror.

Paper 110800 received Jul. 8, 2011; revised manuscript received Nov. 3, 2011; accepted for publication Nov. 10, 2011; published online Jan. 31, 2012.

1 Introduction

Measuring technology has been used to assure the quality and safety of products in manufacturing processes. In particular, three-dimensional (3-D) profiling systems have become essential tools in manufacturing industries.[1] However, conventional 3-D profiling systems have several shortcomings, including being very large in size, heavy in weight, and expensive in price. Consequently, there is a strong demand for an inexpensive, portable camera for 3-D profilometry in industrial applications. There is a need to measure 3-D profiles of products in the automobile, electronic, mechanical, and apparel industries and also in the medical care field.

It is expected that the above requirements can be met by an optical 3-D measurement method based on the pattern-projection method, which is widely used in industrial applications. There are three main methods for performing fringe analysis in pattern-projection techniques: phase-shifting methods, Fourier-transform methods, and space-encoding methods.[1,2] In this study, we adopt a phase-shifting method, which is extensively used in industrial applications. Various pattern-projection techniques have been proposed (see Fig. 1). pattern-projection techniques can be classified into two groups: analog and digital methods. For analog methods, a stepping motor is generally used to move a pattern printed on a glass plate. Digital methods can be classified into those that use a liquid crystal grating (LCG), a liquid crystal display (LCD) and those that employ microelectromechanical systems (MEMS).[3] Methods that use either LCGs or LCDs are a matrix and/or stripe type.[4] In MEMS applications either a digital light processing (DLP)/digital mirror device (DMD)[5–8] or a single mirror is used. Figure 2 depicts optical setups that employ LCD and DLP/DMD projectors. The light source of the LCD projector is a halogen lamp or a LED. Two dichroic mirrors are used to separate red, green, and blue from the white light source. LCDs can independently control the transmitted intensities of the three colors at each pixel. After a cross dichroic prism (X-cube) recombines a programmable pattern of three colors, a periodic pattern can be projected on the surface of a sample. The LCD projector is large and heavy since its optical system contains three LCDs, a cross dichroic prism, and a projection lens. A halogen lamp or a LED is used as the light source for a DLP/DMD projector with one chip. After light passes through a pair of lens units and color filters, it is reflected by the DMD. DMDs can be computer-controlled and they are used as switching devices in the same manner as LCDs. DMDs have faster response speeds than LCDs. DMD projectors have become inexpensive and consequently. Consequently in many studies methods based on DMDs are reported. In particular, some studies have used DLPs to perform rapid 3-D measurements.[5–8]

As an alternative to DLP/DMD technology, we have proposed a 3-D profile measurement method that uses a single MEMS mirror.[9,10] This principle is potentially able to realize a compact camera for 3-D profile measurement since the single MEMS mirror is inexpensive and very small. In this system, a laser diode and an single MEMS mirror are used for pattern-projection. The voltage applied to the laser diode is controlled to generate an appropriate periodic pattern. The key aspect to the projection method is in that a fringe pattern generated in the time domain can be transformed into the spatial domain by the MEMS mirror. We are trying to develop a prototype compact camera for 3-D measurement by incorporating a single MEMS scanner. This paper

0091-3286/2012/$25.00 © 2012 SPIE

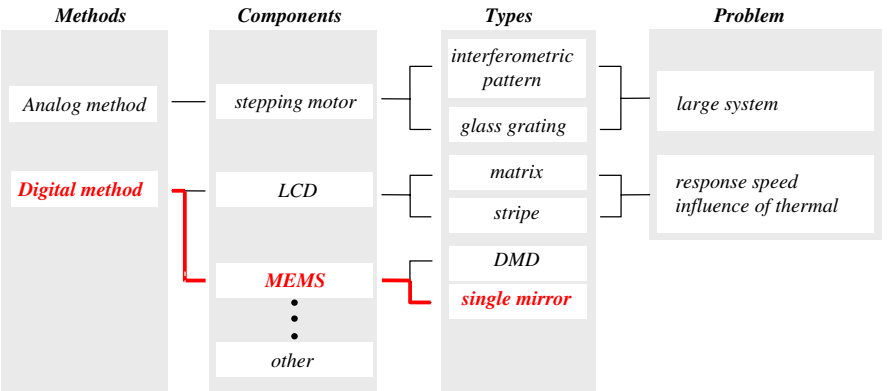

Fig. 1 General classification of pattern-projection techniques. (Color online only.)

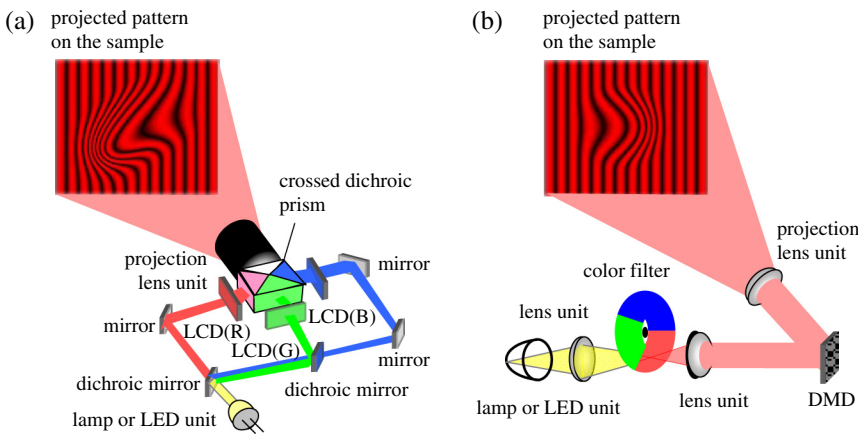

Fig. 2 Optical system using conventional commercial projector; (a) projection technique based on LCDs projector; (b) projection technique based on DLP/DMD projector with one chip. (Color online only.)

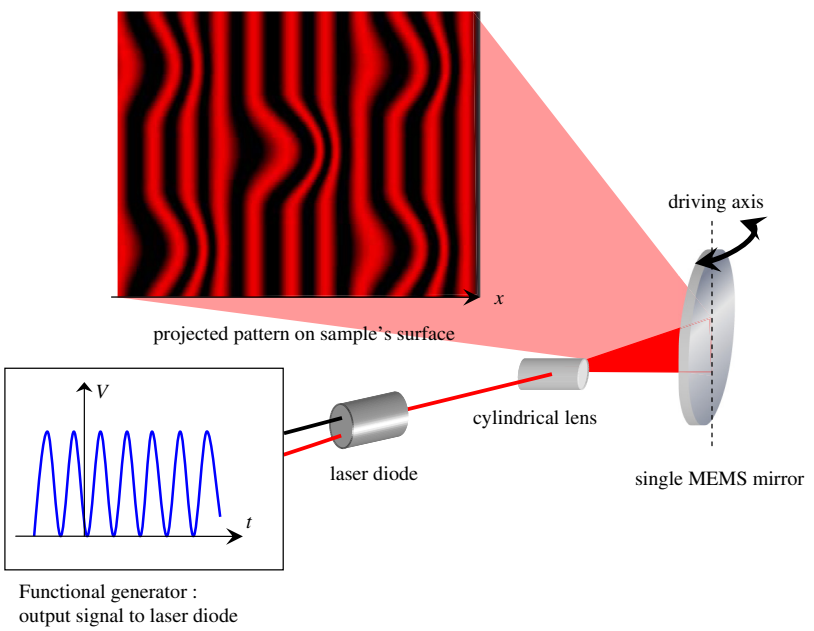

Fig. 3 Projection technique using a single MEMS mirror. (Color online only.)

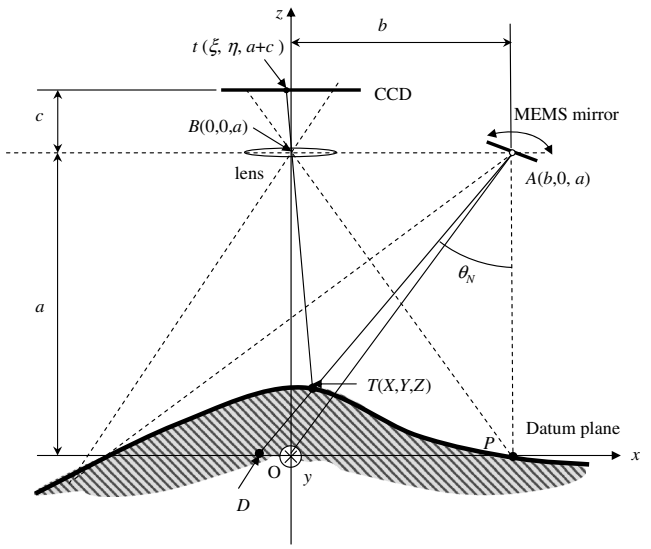

Fig. 4 Optical arrangement for three-dimensional profilometry.

describes the principle and optical configuration of the compact camera along with its basic performance.

2 Principle

2.1 *Pattern Projection Technique Using a Single MEMS Mirror and a Laser Diode*

Figure 3 shows the optical configuration of the pattern-projection technique. We employed a laser diode as a monochromatic light source. The laser beam is converted by a cylindrical lens or a line-generator lens from a line beam to a fan beam. This beam is incident on a single MEMS mirror, which oscillates about its axis to follow the longitudinal direction of the line beam and the driving axis of the single MEMS mirror. The rotation rate of the MEMS mirror is roughly assumed to be constant with time, i.e. a plot of its rotation angle looks like a triangle wave. The fan beam can be used to scan a sample by rotating the single mirror so as to illuminate a two-dimensional area. At the same time, a function generator is used to generate appropriate projected patterns. The pattern can be formed by the input signals controlled by the function generator. In other words, we can convert a projection pattern that contains appropriate periodic structures and an arbitrary intensity distribution, such as a sinusoidal pattern from the time domain to the spatial domain. For fringe analysis, a phase-shifting algorithm can be used to precisely analyze the pattern. To utilize a phase-shifting algorithm, the phase of the input signal applied to the laser diode should be modulated. Shifting of fringe patterns can be achieved by modulating the initial phase of the input signal. By controlling the input signals from the function generator, an appropriate pattern can be generated quickly and precisely.

2.2 *Configuration of Compact Camera for 3-D Profilometry*

Figure 4 shows the optical configuration of a compact camera for 3-D profilometry that incorporates a single MEMS mirror. The projector using the single MEMS mirror shown in Fig. 3 is located at the point $A(b, 0, a)$ in Fig. 4. In the coordinate system (x, y, z) shown in Fig. 4, the lens of a CCD camera is set at the point $B(0, 0, a)$ and the imaging plane of the CCD is set at the distance c from the point B in the z direction. The angle between $\overline{AP}$ and $\overline{AD}$ is denoted by θ_N, where the line $\overline{AP}$ is vertical to the datum plane and N

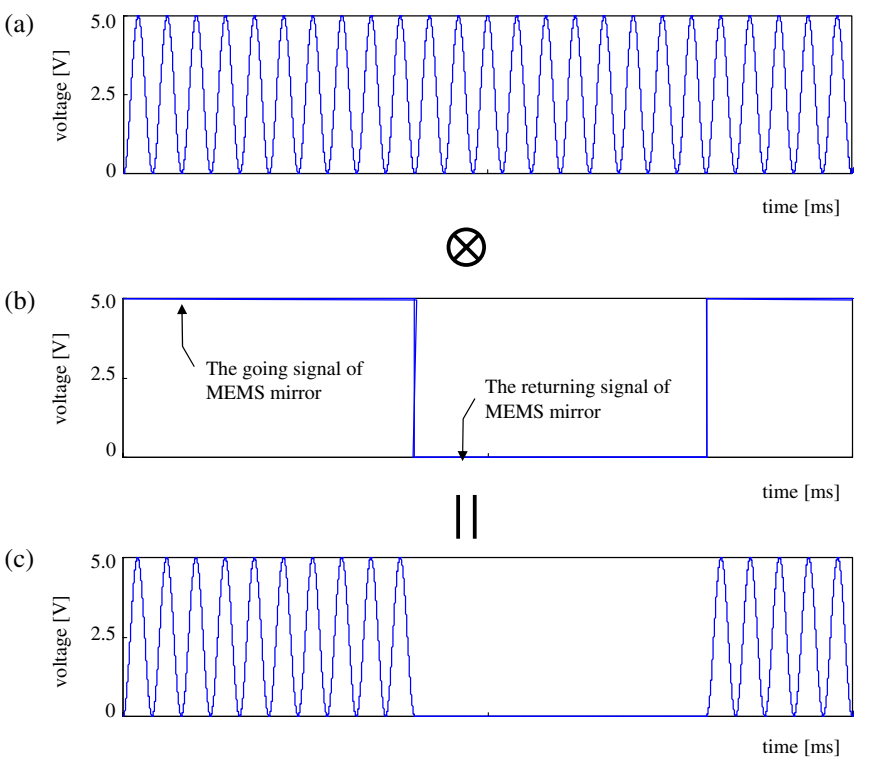

Fig. 5 The relationship of the signals; (a) Signals generated by FG; (b) Reference signals; (c) Input signals to LD. (Color online only.)

indicates the number of fringes. The point $T(X, Y, Z)$ is located on the sample surface. Then, from the geometrical calculation, the point $T(X, Y, Z)$ on the sample surface[4,11] can be expressed by

$$X = \left(\frac{Z-a}{c}\right)\xi, \tag{1}$$

$$Y = -\frac{\sqrt{X^2+(a-Z)^2}}{\sqrt{c^2+\xi^2}} \cdot \eta, \tag{2}$$

$$Z = \left(1 - \frac{bc}{cw - a\xi}\right)a. \tag{3}$$

Here, ξ and η are pixel positions on the CCD plane. Symbol w is as follows:

$$w = \frac{p\phi(\xi,\eta)}{2\pi}. \tag{4}$$

Symbols p and $\phi(\xi,\eta)$ mean the pitch of the fringe pattern and the phase distribution of the fringe, respectively. We can obtain Eqs. (1) and (3) by considering the angle θ_N

$$\tan\theta_N = \frac{w}{a} = \frac{b-X}{a-Z}, \tag{5}$$

and from the relationship of a ratio of similitude between lines $\overline{tB}$ and $\overline{TB}$.

$$X : -\xi = a - Z : c \tag{6}$$

and

$$Y : -\eta = \sqrt{X^2+(a-Z)^2} : \sqrt{c^2+\xi^2}. \tag{7}$$

Here, $\phi(\xi,\eta)$ expresses the sample's phase distribution including height information and θ_0 indicates $\angle PAO$. The intensity distribution $I_i(\xi,\eta)$ can be captured using the CCD camera. A voltage, such as a sinusoidal wave in the time domain, is generated by the function generator and applied to the laser diode. The symbol i indicates the number ($i = 0$, 1, 2, 3) of the intensity distribution captured by the CCD camera. The intensity distribution $I_i(\xi,\eta)$ can be written including the phase distribution $\phi(\xi,\eta)$ as follows,

$$I_0(\xi,\eta) = I'(\xi,\eta) + I''(\xi,\eta)\cos[\phi(\xi,\eta)] \tag{8a}$$

$$I_1(\xi,\eta) = I'(\xi,\eta) + I''(\xi,\eta)\cos[\phi(\xi,\eta) + \pi/2] \tag{8b}$$

$$I_2(\xi,\eta) = I'(\xi,\eta) + I''(\xi,\eta)\cos[\phi(\xi,\eta) + \pi] \tag{8c}$$

$$I_3(\xi,\eta) = I'(\xi,\eta) + I''(\xi,\eta)\cos[\phi(\xi,\eta) + 3\pi/2], \tag{8d}$$

where $I'(\xi,\eta)$ and $I''(\xi,\eta)$ are the bias and amplitude components, respectively. The initial phases of the intensity distribution δ_i ($i = 0$ to 3) are given by 0, $\pi/2$, π, and $3\pi/2$, respectively. The four-step phase-shifting technique can be used to determine the phase distribution $\phi(\xi,\eta)$. Hence, the phase distribution, including the sample's height information, is given by

Fig. 6 Prototype palm-top camera.

$$\phi(\xi,\eta) = \tan^{-1}\frac{I_3(\xi,\eta) - I_1(\xi,\eta)}{I_0(\xi,\eta) - I_2(\xi,\eta)}. \tag{9}$$

The phase distribution is obtained from $-\pi$ rad to $+\pi$ rad with 2π discontinuities. A phase unwrapping algorithm is applied to obtain a continuous phase. Phase unwrapping can remove the 2π discontinuity by adding or subtracting multiples of 2π. After obtaining the continuous phase, the

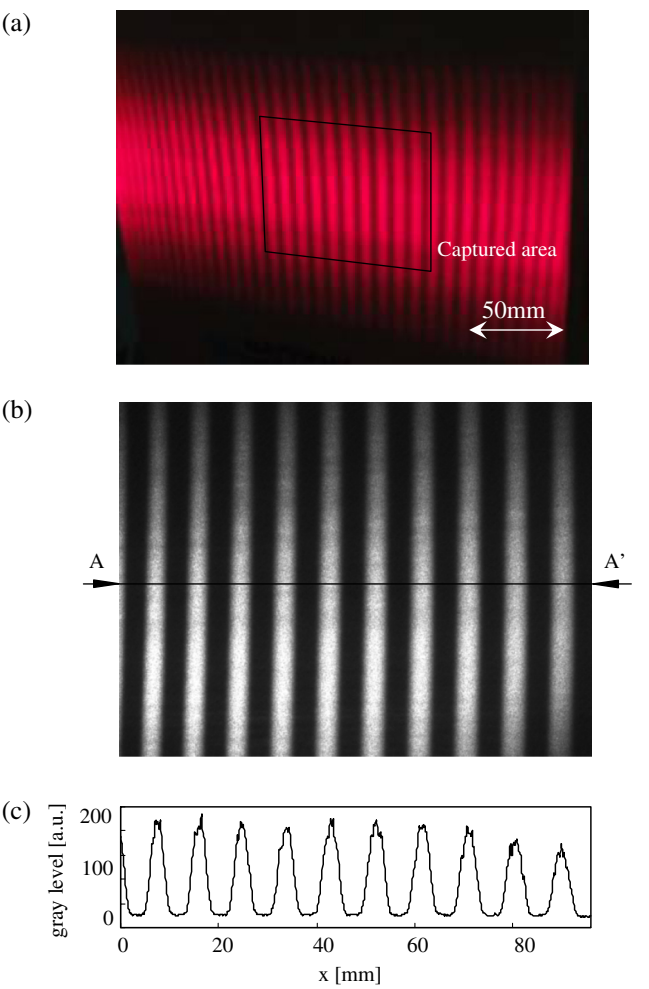

Fig. 7 Projected pattern of proposal method; (a) Projected pattern on paper is captured by a digital photographic camera; (b) Captured image by CCD camera; (c) Intensity distribution of $A - A'$. (Color online only.)

coordinates of the sample (X, Y, Z) can be determined from Eq. (1) to (9).

3 Experimental Setup and Results

The optics of the projection system uses a laser diode (ADL66z01-HU, Arima Co. Ltd.) as the light source and a resonance scanner (LSM 500, Venture Forum Mie Ltd.) as the single MEMS mirror. It also uses an aspheric collimator lens ($f = 11$ mm) and a cylindrical plano-convex lens ($f = 250$ mm). The laser diode has a wavelength of 660 nm and a nominal maximum output power of 60 mW. The laser diode and the resonant scanner have dimensions of $\phi 14$ mm $\times$ 62 mm(L) and $\phi 10$ mm $\times$ 12 mm(L), respectively. The single MEMS mirror in the resonant scanner is 3 mm in diameter and has a sympathetic vibration frequency of 500 Hz. The MEMS mirror can be restored to its original position by applying 0 and 5 V signals during the going and returning cycles. During the going cycle, a voltage generated by the function generator is applied to the laser diode, whereas the laser diode is switched off during the returning cycle. Figure 5 shows signals between the single MEMS mirror and the function generator. Figures 5(a) and (b) show the signal generated by the function generator and the signal that specifies the going (5 V) and returning (0 V) directions of the single MEMS mirror. The combined signal shown in Fig. 5(c) is applied to the laser diode. The projected pattern can be phase-shifted by modulating the initial phase of the signals as shown in Fig. 5(a). As mentioned above, this projection system can sweep the projected pattern at the rate of 500 Hz. It is theoretically possible to modulate the projected pattern up to the maximum frequency of the MEMS mirror (i.e., from 2 to 8 kHz).

Figure 6 shows the compact camera developed for 3-D profilometry, which has dimensions of 53 mm $\times$ 130 mm $\times$ 38 mm and a weight of 320 g. A compact CCD camera (STC-RCL33A, Sentech Co., Ltd.) with an 8-bit gray scale in monochromatic use is employed. The camera lens has a focal length of 16 mm. The CCD camera is positioned on the left of the camera and the single MEMS mirror is set on the right. The bandpass interference filter (wavelength $\lambda_0 = 656$ nm; FWHM (full width at half maximum): 10 nm; Edmund Optics Ltd.) is mounted in front of the camera lens and an optical window is installed in the front of the MEMS mirror. The distance a and the baseline length b shown in Fig. 3 are 100 and 250 mm, respectively. Although the maximum output power of the laser diode is 60 mW, the output of the beam from the compact camera is reduced to 3 mW by the influence of the input generated signals. The scanning angle of the MEMS mirror is as wide as 40°. The illumination area is 100 mm(H) $\times$ 180 mm(W) at the object distance of 250 mm. The effective imaging area is 75 mm(H) $\times$ 90 mm(W) in Fig. 7(a); this area was selected since it is suitable for measuring a small car component and as the pattern period decreases at both ends of the imaging area.

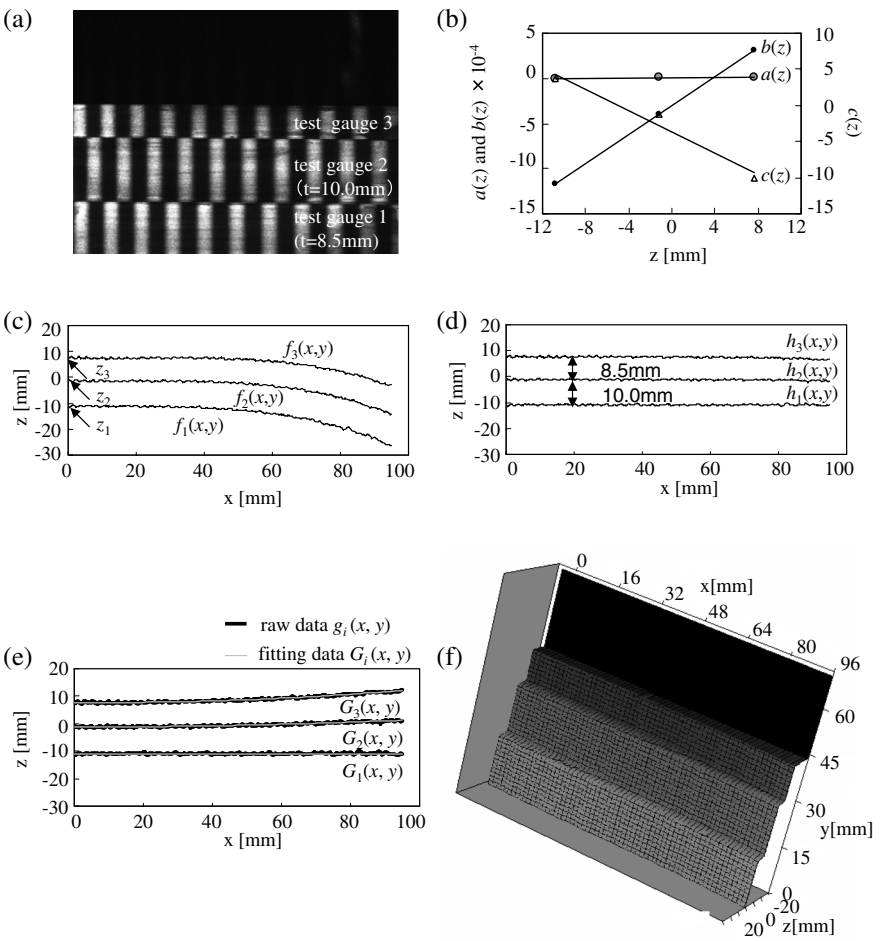

Fig. 8 Three-dimensional profile of test reference gauge; (a) Projected pattern of the standard; (b) Measured raw data; (c) $g_i(x, y)$ and $G_i(x, y)$; (d) The relation ship of the parameters $a(z)$, $b(z)$ and $c(z)$; (e) Calibrated data after calibration; (f) 3-D profile.

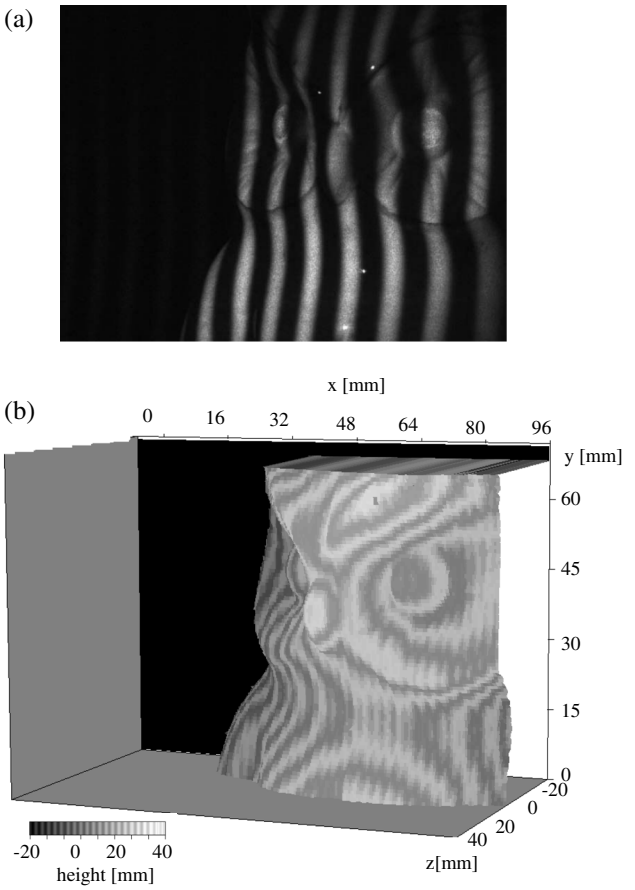

Fig. 9 Three-dimensional profile of pottery of the owl; (a) original image; (b) 3-D image.

Therefore, the center area of the projected pattern is utilized to measure the surface profile to reduce the error in the driving speed of the MEMS. We are currently attempting to overcome this problem by using a special lens that intentionally adds aberration. In this paper, we solved this problem by measuring the limited area shown in Fig. 7(a) and performing a calibration. Figure 7(b) shows a raw image captured by the CCD camera incorporating this compact camera. The intensity distribution has very clear contrast, as shown in Fig. 7(c). At this stage in development, the control unit for the laser diode, the MEMS scanner, the CCD camera, and the function generator circuit are separated from the camera unit. A sinusoidal voltage ($f = 40$ kHz; $E = 0$ 5 V) is applied to the laser diode. The CCD camera is connected to a notebook computer (CF-Y8, Panasonic Co., Ltd., Intel (R) Core (TM) 2 Duo CPU L7800@2.00 GHz, 777 MHz, 1.99 GB RAM) by a camera capture card (Frame Link VCE-CLB01, Imperx Co., Ltd.) The phase shift of the projected pattern has a time lag of 0.5 s so that it takes 2.0 s to capture four images. The time between capturing an image and displaying it is 3.0 s due to the time taken for analyzing the image.

Reference samples were used to evaluate the performance of this compact camera for 3-D measurements. Three test gauges were arranged in a step-like arrangement with intervals of 10 and 8.5 mm between the steps. Figure 8(a) shows an original image of the projector for the reference sample. A periodic pattern is projected with a large period relative to the steps of the test gauges for avoiding 2π ambiguity of phase distribution. The surface profile is determined using a four-step algorithm. Figure 8(b) shows the cross-sectioned profile of the test gauges. Although a flat section was measured, the measured raw data shows a curved section. The calibration method can correct for the variation in the speed of the MEMS mirror. Here, three data of the cross sectioned profile in Fig. 8(b) are defined $f_1(x, y)$, $f_2(x, y)$ and $f_3(x, y)$, respectively. The data is conducted to calculate as follows.

$$\alpha(x, y) = f_1(x, y) - z_1. \tag{10}$$

Here, z_1 indicates the height shown in Fig. 8(b). After fitting $\alpha(x, y)$ by the cubic polynomial expression, we can obtain

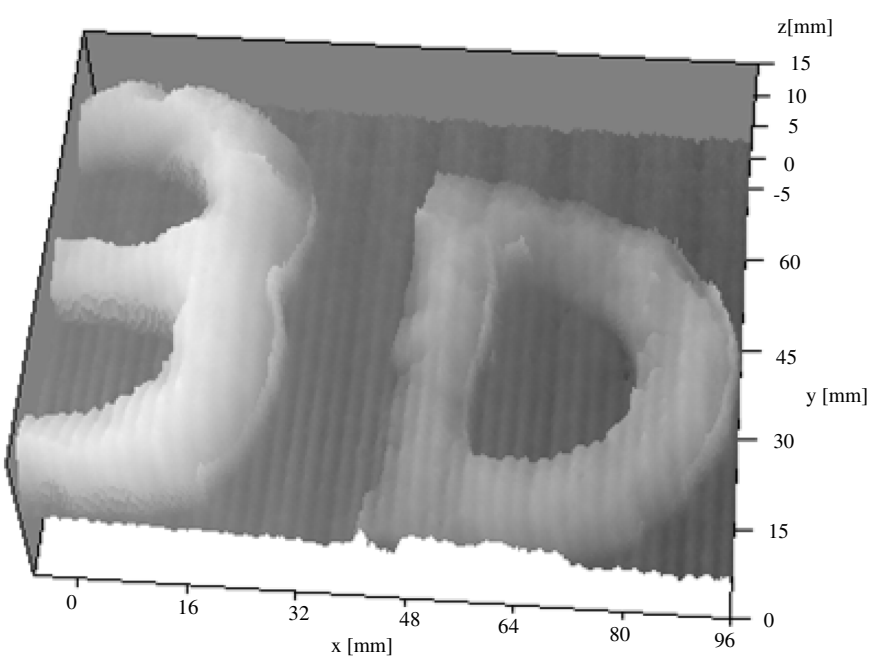

Fig. 10 Three-dimensional profile of test sample.

the fitting function $\beta(x,y)$. The function $g_i(x,y)$ is given by subtracting $\beta(x,y)$ from $f_i(x,y)$

$$g_i(x,y) = f_i(x,y) - \beta(x,y). \tag{11}$$

Although the data shown as $g_1(x,y)$ becomes a flat along x axis, it is clear that the coefficients of a quadratic function shown $g_2(x,y)$ and $g_3(x,y)$ are different, respectively. To calibrate the variation in the speed of the MEMS mirror, we calculate the coefficients of a quadratic function shown as $g_2(x,y)$ and $g_3(x,y)$, respectively. After fitting $g_i(x,y)$ by the quadratic polynomial expression, we can determine the fitting function $G_i(x,y)$ in Fig. 8(c). The function $G_i(x,y)$ can be expressed as

$$G_i(x,y) = a_i \cdot x^2 + b_i \cdot x + c_i. \tag{12}$$

In this optical arrangement, we can obtain three parameters a_i, b_i and c_i shown in Fig. 8(d). All parameters a_i, b_i and c_i can be fitted by the linear polynomial expression as follows

$$a_i = a(z) = 0.67 \times 10^{-6} \cdot z + 73.2 \times 10^{-6} \tag{13a}$$

$$b_i = b(z) = -58.9 \times 10^{-6} \cdot z - 591 \times 10^{-6} \tag{13b}$$

$$c_i = c(z) = 1.00 \cdot z - 0.10 \times 10^{-3}. \tag{13c}$$

Since the parameters a_i, b_i and c_i change along z axis, $a(z)$, $b(z)$ and $c(z)$ can be represented as the function of z. Finally, the data of the cross-sectioned profile after the calibration can be determined as follows.

$$z(x,y) = h_i(x,y) = g_i(x,y) - \{a(z) \cdot x^2 + b(z) \cdot x\}. \tag{14}$$

According to the calibration method, we can calibrate the influence of the speed of the MEMS. As a result, Fig. 8(e) can be given as the calibration results. The measured results became a straight line and there were variations of about 0.3 mm. Here, variations represented the mean error and the maximum error to be about 0.5 mm. To achieve the high accuracy measurement, we have only to project the fine periodical pattern. Figure 8(f) shows 3-D surface profile of the test pieces.

As an example, we measured a ceramic owl which, despite its glazed pottery, has a projected pattern with a very high contrast. Figure 9(b) shows a 3-D image of the owl. The gray level and contours indicate the height of this ceramic owl. Figure 10 shows another example in which the character's "3-D" are carved. Figures 8, 9 and 10 show the relevant contour patterns. The effect of the contour pattern is replicated at quadruple its frequency onto the surface height map as the fringe pattern is not an imperfect sinusoidal wave. The magnitude of the contour patterns was up to 0.5 mm. If we calibrate the laser output relative to the input signal, the contour pattern will be deleted.

4 Conclusions

We developed a compact camera for 3-D profilometry using a single MEMS mirror and a laser diode. We demonstrated its performance and potential for applications. The key technology to this measurement is a single MEMS mirror for pattern-projection and does not use a DLP or an LCD. The 3-D camera is as compact as a conventional digital camera and can shift the phase of projected patterns by several milliseconds. Moreover, this projection method can shift appropriate periodic patterns by in an arbitrary period. A laser diode is employed as the light source and no projection lens is used in this system. This 3-D camera imposes no limitations on the size of the measurement area that is caused by distortion of the projection lens. Based on the above-mentioned advantages, this instrument is expected to be utilized for many practical applications in various industries. In the future, we intend to construct a more compact 3-D camera built in an electric circuit.

References

1. T. Yoshizawa, Ed., *Handbook of Optical Metrology, Principles and Applications*, CRC Press, New York (2009).
2. M. Takeda, H. Ina, and K. Mutoh, "Fourier-transform method of fringe-pattern analysis for computer-based topography and interferometry," *J. Opt. Soc. Amer.* **72**, 156 (1982).
3. M. J. Baker et al., "A contrast between DLP and LCD digital projection technology for triangulation based phase measuring optical profilometers," *Proc. SPIE* **6000**, 60000G (2005).
4. K. Yamatani et al., "Three-dimensional surface profilometry using structured liquid crystal grating," *Proc. SPIE* **3782**, 291–297 (1999).
5. P.S. Huang, S. Zhang, and Fu-Pen Chiang, "High-speed 3-D shape measurement based on digital fringe projection," *Opt. Eng.* **42**, 163–168 (2003).
6. P.S. Huang and S. Zhang, "Fast three-step phase shifting algorithm," *Appl. Opt.* **45**, 5086–5091 (2006).
7. S. Zhang, "Recent progresses on real-time 3-D shape measurement using digital fringe projection techniques," *Opt. Laser Eng.* **48**, 149–158 (2010).
8. G. Abramovich and K. Harding, "A hand held triangulation sensor for small features measurement," *Proc. SPIE* **7855**, 78550F (2010).
9. T. Yoshizawa, T. Wakayama, and H. Takano, "Applications of a MEMS scanner to profile measurement," *Proc. SPIE* **6762**, 67620B1–8 (2007).
10. T. Yoshizawa and T. Wakayama, "Compact camera system for 3-D profile measurement," *Proc. SPIE* **7513**, 751304 (2009).
11. T. Yoshizawa and K. Suzuki, "Automated 3-D measurement of shape by grating projection method," *J. Jpn. Soc. Prec. Eng.* **53**(3), 422–426 (1987) in Japanese.

Toshitaka Wakayama received his BS, MS and PhD degrees in Mechanical Systems of Engineering from Tokyo University of Agriculture and Technology, Japan. He joined Saitama Medical University as a research associate in 2006, and is presently an assistant professor. His current research interests are optical engineering, imaging metrology and biomedical photonics.

Toru Yoshizawa received his BS, MS and Doctor of Engineering degrees in precision engineering from the University of Tokyo. After 10 years of research and educational work at Yamanashi University, he moved to the Tokyo University of Agriculture and Technology, where he was professor in the Department of Mechanical Systems Engineering for 25 years. After retirement from this university, he worked in industry for three years and again moved to Saitama Medical University to initiate the Department of Biomedical Engineering. Currently he is part-time professor in this department of the Saitama Medical University and Professor Emeritus at the Tokyo University of Agriculture and Technology. At the same time, he is leading the Non-Profit Organization "3-D Associates". His research field covers optical metrology, inspection, and optomechatronics.